

# TRADEOFF BETWEEN TOTAL HARMONIC DISTORTION AND EFFICIENCY IN COUPLING OF A CLASSICAL BRIDGE INVERTER AND A PHOTOVOLTAIC SYSTEM

Lucas F. Aguiar, Emerson Grzeidak, João Paulo C. L. da Costa and Rafael A. Shayani

University of Brasilia, Brasilia (Brazil)

## 1. Introduction

The diary availability of solar energy, the benefits of clean and renewable energy and the crescent tendency of distributed generation contribute to fast advance of photovoltaic systems. The process of energy generation with solar cells is in a continuous evolution, reaching each year higher levels of efficiency, which combined with the advancements in the power electronics field and semi-conductors technology in large scale production makes the utilization of the photovoltaic systems cheaper and more efficient. Therefore, investments in solar energy supplied houses, buildings, industries and transportation increase. Fig. 1 illustrates the cumulative growth in PV capacity in major solar energy producing countries from 1992 to 2009 (IEA PVPS Programme, 2009).

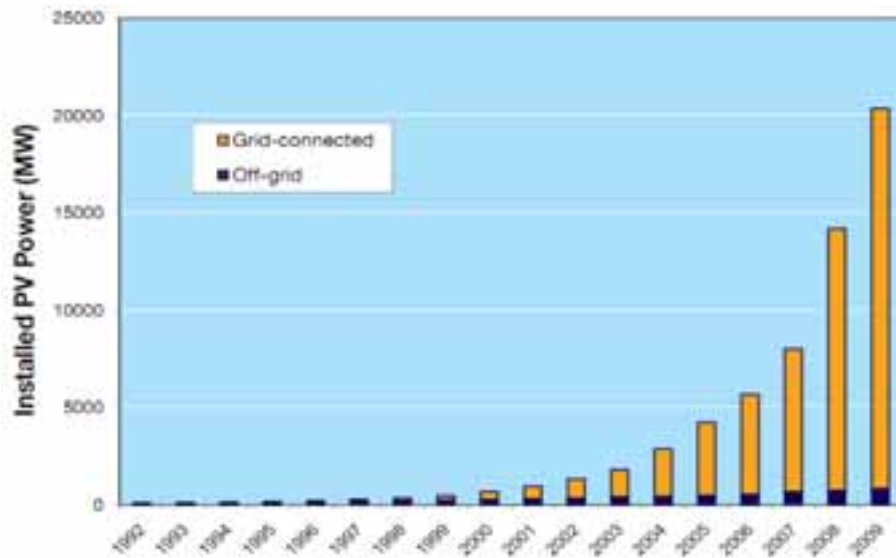


Fig. 1: Cumulative installed grid-connected and off-grid PV power in IEA countries (IEA PVPS Programme, 2009)

Once PV systems generate direct current (DC) signals, it is necessary to convert it to alternating current (AC) signals by applying an inverter. Inverters are used in a wide range of applications, from small power supplies for a computer to large industrial applications to transport bulk power. When applied to PV systems the DC power produced by the PV generator is converted into AC power. AC power is necessary in PV systems because the majority of the loads are AC. Therefore, the inverter is one of the key components of connecting the PV systems either to the grid or to off-grid systems as cited in Amrouche et al. (2007).

The converted AC signal is delivered to an off-grid system, which is useful to both domestic purposes and non-domestic installations, providing electricity to households, villages and rural areas that are not connected to the utility grid as shown in Claverie et al. (1994); Muljadi (1997); Hamidat et al. (2002); Schinca and Amigo (2010); Misak et al. (2011); Ranjit et al. (2011). The energy produced is also applied for lighting, refrigeration, telecommunication, water pumping and more specific applications such as vaccine refrigeration and other low power loads (Ofualagba, 2008).

The off-grid system has an important characteristic, its modularity, in other words, it is built out by several parts or components. A basic off-grid system has a PV module, a rectification section, a conversion or inversion section and a load. Besides that, it is common the utilization of a battery as energy storage and a charge controller. An interface circuit, which can be composed either by a rectifier, an inverter, a battery, a resonant circuit, among others, coupled between the PV module and the load is necessary to increase the system efficiency, smoothing the oscillations of the energy supplying by the PV cells due to the solar irradiance and temperature changes (Castaner and Silvestre, 2002).

In this paper, an off-grid system designed to feed either rural houses or villages using self-regulating photovoltaic panels is simulated. In order to achieve a low cost system, the scheme in Fig. 2 composed of PV modules, battery, inverter and resonant circuit is considered. Notice that the charge controller is not included. In this paper, both THD and Efficiency analysis of a Resonant Circuit coupled to the output of one of the most popular inverter topology, known as classical full-bridge, is performed. Full-bridge topology has recently been applied in works involving inverters (Feel-soon, K. et al., 2005; Banaei, M.R. and Salary, E, 2011; Colak, I. et al., 2011). The reason for choosing this topology is its simplicity, low cost and reasonable efficiency, which results in a good cost-benefit relation so that this system can be utilized to produce energy in places far from the public electric network. In these places, energy is used for simple applications such as lighting, heating and water pumping, in order to ensure the minimum of comfort quality of life for these people. This topology also permits to generate both Square-Wave, or Modified-Square Wave or Enhanced-Modified-Square-Wave. PWM-based wave is not considered in the subsequent analysis because it requires more complex circuits, which are expensive.

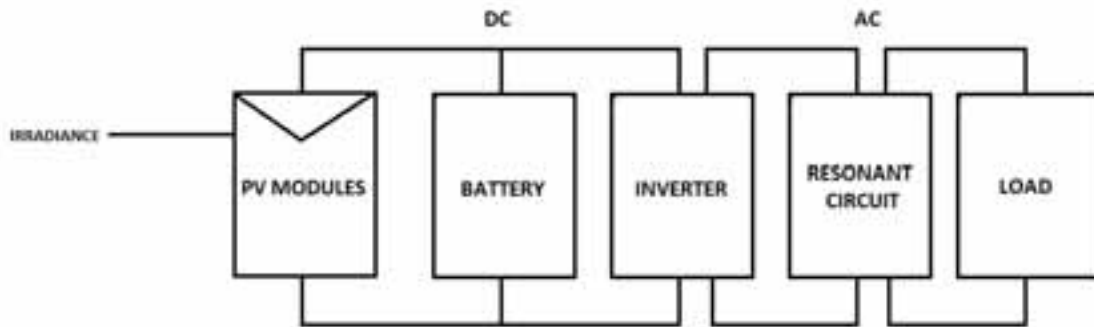


Fig. 2: Off-grid system

Since most of the PV System components are described by non-linear equations and the resulted equations of the node analysis most often do not have analytic solutions, computational ancillary is indispensable. Besides that, simulating real solar irradiance profiles in order to obtain accurate results closer to reality is possible. All simulations are based in a robust model that considers a wide range of variables in order to be closer to the reality. Real data is used in the modeling. In the following sections the means to replicate the models are provided, but for more information about models of PV modules, battery, and inverter, the reader is referred to Castaner and Silvestre (2002).

Off-grid systems, whether fed by non-sinusoidal wave based inverters, generate harmonics in current that may cause damages to the load. Coupling a resonant filter between an off-grid system and the load is an affordable way to reduce harmonic distortions. The goal of this procedure is to obtain a sine wave with 60 Hz in order to reduce the Total Harmonic Distortion delivered to the load, as discussed in Cho, K.M et al. (2003). On the other hand, it may also decrease the system efficiency. Therefore, it is necessary to find out a tradeoff between both THD and Filter Efficiency.

There are some regulatory technical standards for the THD for both current and voltage, but we chose the most used, that is the IEEE standard (IEEE 519, 1992). IEEE 519 (1992) establishes 5% of THD for the output voltage as maximum to be inserted by a general system in order to prevent from creating power system problems.

This article describes a basic explanation about the system structure, but the main goal of this paper is to find out a relationship between the Total Harmonic Distortion (THD) and the efficiency of the resonant filter utilized. Three different non-sinusoidal inverters and its problems are analyzed before and after the filtering process. Many system variables involved are considered in order to perform a reliable analysis.

The remainder of this paper is organized as follows. In Section 2, it is showed how the Resonant Circuit Input Signals were obtained. Considerations about both the irradiance profile, the behavior of the PV modules model, the battery model and the inverter used in this work are made in this section. Section 2 has the goal of contextualizing the subsequent analysis to reality. Section 3 is reserved for sizing the Resonant Circuit. In section 4, the method of analysis used in this paper is presented, including the definition of Total Harmonic Distortion and Efficiency. Section 5 is dedicated to an important result involving THD and Q-factor. In Section 6, a relationship between Efficiency and Q-factor is analyzed. Section 7 comes up with a discussion about THD and Efficiency for the Resonant Filter. Section 8 shows the conclusion.

## 2. Resonant Circuit Input Signal

The irradiance is defined as the integral of spectral irradiance extended to all wavelengths of interest. Since radiation of the sun reaching the earth is partly reflected by the atmosphere and partly transmitted to the earth's surface, the irradiance varies from day to day. Therefore, it is necessary to consider an irradiance profile of a given day.

This article uses a real irradiance profile for terrestrial PV applications. All data was acquired by the Renewable Energy Sources Laboratory, of the Electrical Engineering Department of the University of Brasilia, Brazil, in 2006. Fig. 3 presents the irradiance profile obtained.

The irradiance profile is the data input of the model. The PV model requires that the irradiance profile is modeled as a voltage source, so that the voltage delivered by PV modules can be simulated. Two arbitrary cloudy days that represent normal weather conditions were chosen. Since the focus of the paper is not in the PV models, this consideration is good enough for our purposes.

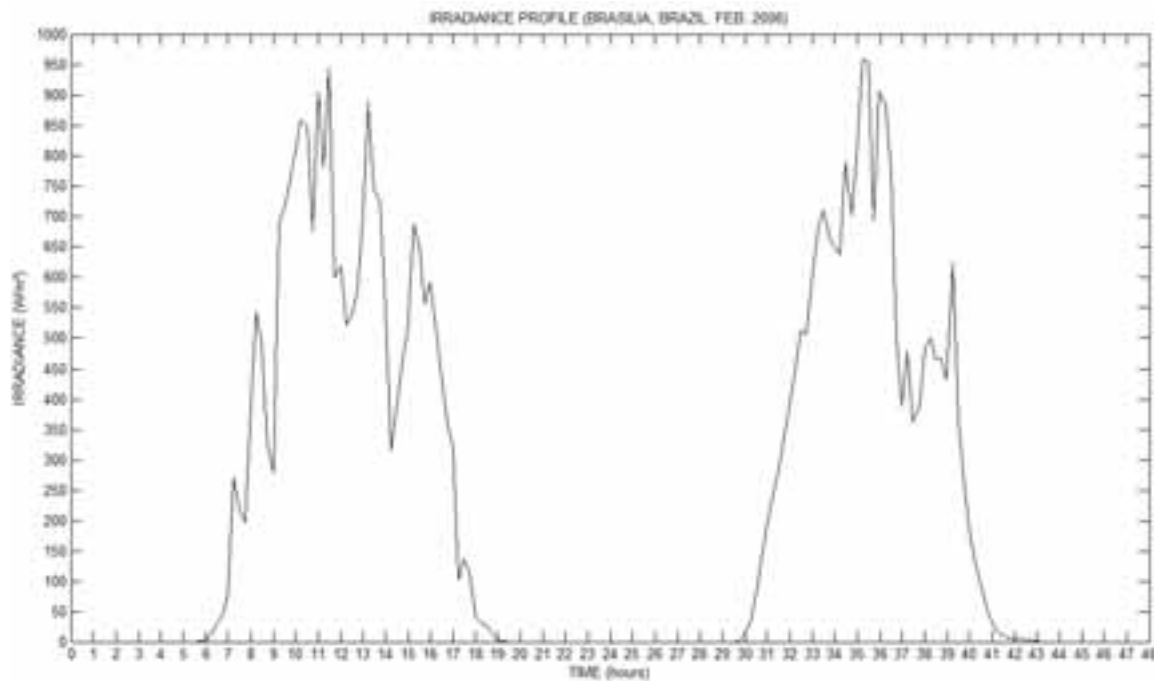


Fig. 3: Irradiance Profile

The whole system was modeled based in real data in order to be realist. In this section, all the variables considered in the simulations are present.

### 2.1. PV Modules Model

Lead-acid batteries require at least 14,2V in its terminals so that they can be recharged. Therefore, the PV module has to generate greater voltage to compensate losses. For this purpose it is possible to use either typical panels or self-regulated panels, but when using typical panels it is mandatory to couple a charge controller to avoid battery overvoltage and the consequent evaporation of its electrolyte. Therefore, we decided to use self-regulated panels, which do not need a charge controller because its open circuit voltage is lower than the typical panel's one, so it can be direct connected to the batteries.

On the other hand, there are two constraints in using self-regulated panels. First, self-regulated panels only should be connected to small systems with well-defined load. Second, the battery must be used daily to avoid the PV module to send current to the battery when it is already completely charged. However, these restrictions are not a problem because the proposed system is designed to feed either rural houses or villages, which daily need electricity and do not vary constantly the way they use electricity.

In this analysis, a self-regulated polycrystalline module with 32 cells, KC45 Kyocera model in a parallel array is used. Its voltage coefficient is  $-8.24 \times 10^{-2} V/C^\circ$ , the short-circuit current is 3.1 A, the open-circuit voltage is 19.2 V. The output power of each panel is 45 W. The ambient temperature is 25 °C.

A PV module can be described by the basic equations of a solar cell so that it can be modeled by an electrical circuit (Castaner and Silvestre, 2002). In the model “module\_beh.cir” for the software PSpice (Castaner and Silvestre, 2002), several variables are included, such as series and shunt resistive losses, recombination losses, and temperature effects. Its entry is the irradiance profile showed in Fig. 3 modeled as a voltage signal. The equivalent circuit that models PV cells takes into account an ideal behavior of a solar cell based on an ideal diode and an ideal current source. The responses of the PV panels are greatly consistent.

## 2.2. Battery Model

Lead-acid batteries are the most commonly used energy storage elements for standalone photovoltaic systems because they are affordable and have high storage capacity. However, it is difficult to model these batteries and the estimation of the battery state of charge value is recognized as one of the most complex tasks. The battery used in this paper is of this type. The battery simulation parameters were set according to the lead-acid battery that is coupled to the PV panels installed in the Renewable Energy Sources Laboratory. The model parameters are:

- Nominal Capacity ( $C_{20}$ ): 63Ah. It is the total charge that the battery can store. Usually, this parameter is given by measuring the charge delivered by the battery certain period of time at a given discharge rate and temperature. The subscripted index is the discharge period.
- Initial State of Charge ( $SOC_1$ ): 100%.
- Maximum State of Charge ( $SOC_m$ ): 1872Wh. Maximum battery energy.
- Number of 2V series cells ( $n_s$ ): 6.
- Charge/discharge battery efficiency (K): 0.95. It is a dimensionless number characteristic of the battery (IEEE 1361™, 2003).
- Battery self-discharge rate (D):  $1.48 \cdot 10^{-4} h^{-1}$ . It is also a dimensionless number that depends on the battery characteristics (IEEE 1361™, 2003).

In Fig. 4 is shown the battery voltage evolution given by the simulation when coupling the PV modules and the battery modeled above connected to a  $4\Omega$  resistance in parallel to simulate a continuous loss of energy. The simulation considers the irradiance profile for the two days mentioned in Section 2.

As showed in Fig. 4, the voltage signal delivered to the inverter is approximately 13 V DC.

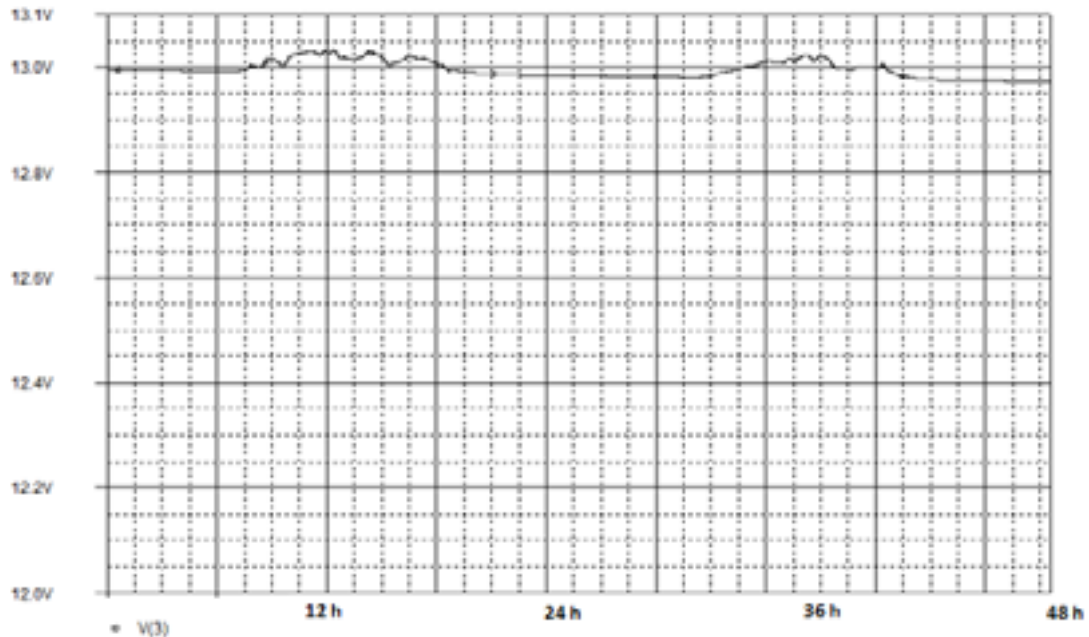
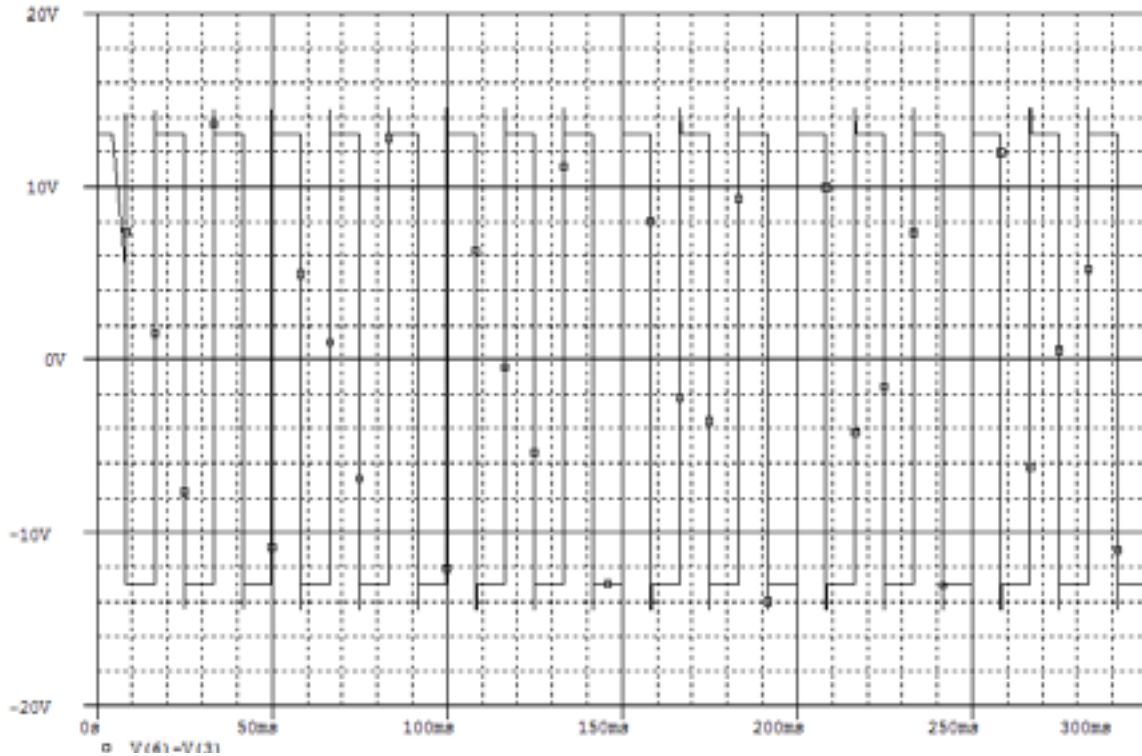


Fig. 4: Battery voltage evolution

Photovoltaic modules provide a direct voltage with small ripples at its output, and for that reason the signal needs to be rectified. After, an inverter is used to transform the signal in an AC wave. There are many inverter topologies, each one with its particular characteristics of losses, size, price, and output signal quality. Basically,

an inverter uses oscillators or more complex control systems coupled to transistors, or similar components, like thyristors or IGBT's, that interrupts a continuous input signal to create the desired wave (Dugan et al. 2002).

Classical Full Bridge is the most widely inverter topology. It is possible to utilize this topology to generate a wide range of waveforms, such as Square-Wave, Modified-Square-Wave or Enhanced-Modified-Square-Wave. The output voltage of the inverter designed to generate a Square-Wave when it receives the input presented in Fig. 4 is showed in Fig. 5.



**Fig. 5: Square-Wave obtained in the simulation**

Following the procedure specified in this section and using variations of the classical full-bridge inverter it is possible to obtain either a Modified-Square-Wave or an Enhanced-Modified-Square-Wave with the voltage amplitude equal to the Square-Wave amplitude, showed in Fig. 5. Wave based in PWM control is not considered in the subsequent analysis because it requires more complex circuits that are expensive. The inverter output signal is delivered to the resonant circuit, which is detailed discussed below.

### **3. Resonant Circuit**

Six parameters are considered in the analysis, some of them are the circuit components and the others are wave parameters. They are summarized below.

- $R$  – resistance of the RLC filter;
- $L$  – inductance of the RLC filter;
- $C$  – capacitance of the RLC filter;
- $Q$  – quality factor (selectivity) of the RLC filter;
- THD – total harmonic distortion of the considered signal;
- $\eta$  – efficiency of the filter.

The resonant circuit is sized to work as a band-pass filter. It is built out using a RLC series connected circuit, with unity power factor. The resonance frequency ( $f_r$ ) is chosen to be 60 Hz because this is the utility grid frequency in Brazil, so that only the signal components with frequencies near to the resonance frequency are allowed to pass, the rest is suppressed.

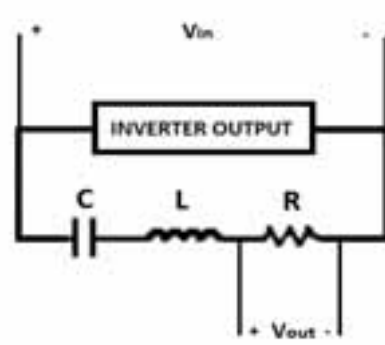


Fig. 6: RLC filter

The following equations are used for sizing the filter:

$$Q = 2\pi f_r \frac{L}{R} \quad (eq.1)$$

$$f_r = \frac{1}{2\pi\sqrt{LC}} \quad (eq.2)$$

Following the Fourier series approach, a periodic function can be written as a sum of sinusoidal functions which are known as harmonics. Harmonic frequencies are multiples of the function original frequency. Therefore, if a periodic wave is submitted to a band pass filter with a cutoff frequency equal to the frequency of the original signal then the output wave will be the fundamental harmonic because the other harmonics will be suppressed.

Total harmonic distortion (THD) is a relation that quantifies the harmonic disturbance. It is given by the equation 3.

$$THD = \frac{\sqrt{\sum_{n=2}^{\infty} V_n^2}}{V_1} \quad (eq.3)$$

In eq. 3,  $V_1$  is the rms value of the first harmonic, and  $V_n$  are the rms values of the nth harmonics.

The filter efficiency can be calculated as the ratio between the output power and the input power, as depicted in the equations below (eq. 4-6).

$$P_{out} = \frac{V_{out}^2}{R} \quad (eq.4)$$

$$P_{in} = \frac{V_{in}^2}{R} \quad (eq.5)$$

$$\eta = \frac{P_{out}}{P_{in}} \quad (eq.6)$$

In both eq. 4 and 5, the mentioned voltage values are rms values. For obtaining the efficiency of the whole system it is necessary to multiply the filter efficiency by both the inverter efficiency, the battery efficiency, and the PV modules efficiency.

After obtaining THD and Filter Efficiency it is necessary to connect these analysis parameters to the filter parameters. The Transfer Function of a Resonant Filter is completely characterized by both Q-factor and its resonant frequency ( $f_r$ ), which in this case is 60 Hz. Therefore, the analysis parameters must be parameterized by Q-factor.

#### 4. Method of Analysis

According to both eq. 1 and eq. 2 there are basically two ways to vary the Q-factor: the first one is to keep the resistance value ( $R$ ) as a constant and then to vary both the inductance value ( $L$ ) and the capacitance value ( $C$ ). The second way is to keep both the inductance and the capacitance values as constants and then to vary the resistance value. Since both inductance and capacitance determine the resonant frequency, the choice was the second one. Both inductance and the capacitance are maintained constants and then the resistance value is calculated to each Q-factor by the eq. 1.

Therefore, in order to establish a relationship between both THD and Filter Efficiency and Q-factor of the resonant circuit, the following method of analysis is used:

First: the waveform delivered to the resonant filter is defined, it can be either Square-Wave, or Modified-Square-Wave, or Enhanced-Modified-Square-Wave. The voltage signals are generating using the first 120 Fourier series components, as showed in Fig. 8 and 9.

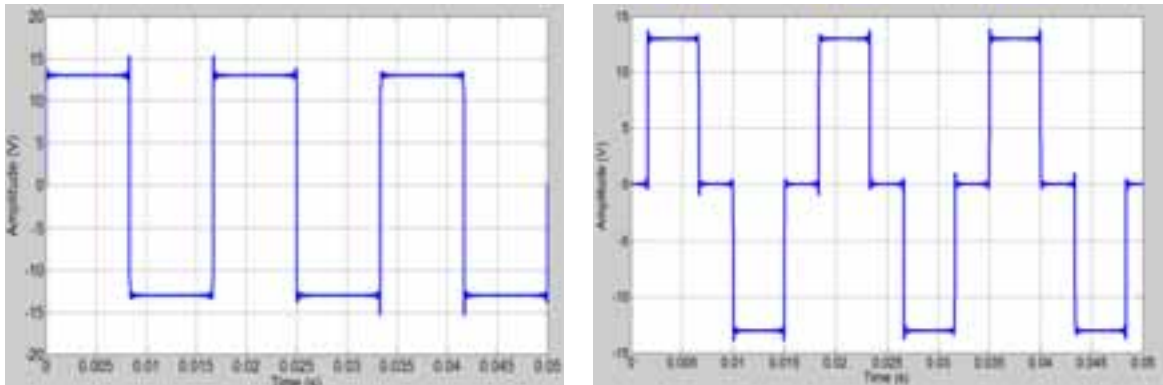


Fig. 8: Square-Wave and Modified-Square-Wave, respectively

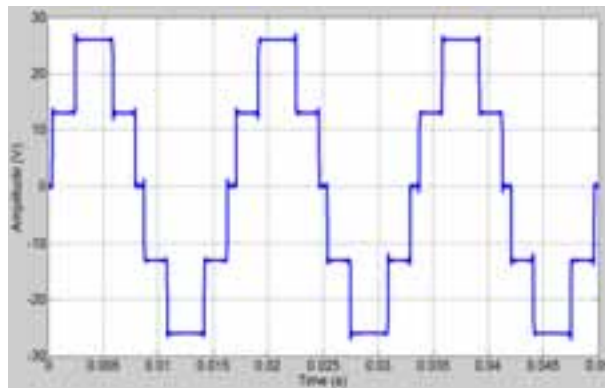


Fig. 9: Enhanced-Modified-Square-Wave

Second: The THD of the original wave is calculated. Table 1 presents those values.

Tab. 1: THD for the original waveforms

Waveform	Square-Wave	Modified-Square-Wave	Enhanced-Modified-Square-Wave
THD	48.13%	36.14%	20.51%

Third: both inductance ( $L$ ) and capacitance ( $C$ ) are chosen. Next, the Q-factor is chosen. Then, the resistance ( $R$ ) is calculated for a 60 Hz resonance frequency using eq. 1. Therefore, the resonant filter is totally determined.

Fourth: the filter transfer function is calculated for a range of Q-factor. Next, the filter input is multiplied by the transfer function of the resonant filter.

Fifth: the THD for the filter output voltage is calculated for each filter determined.

Sixth: the filter efficiency for each filter determined is calculated by eq. 4-6.

## 5. THD and Q-factor

Selectivity is another denomination for Q-factor because the higher this factor the lower the band-width accepted by the resonant band-pass filter characterized by this factor, in other words, more harmonics are suppressed for bigger values of Q-factor. Therefore, it is expected that occurs a reduction of THD levels when filtrating a signal in 60 Hz. Fig. 7 depicts the THD falling for the selectivity increase for the filtered signals. To generate the mentioned graphic the method of analysis described in Section 4 is utilized.

It is possible to notice from Fig. 7 that for small values of Q-factor it is necessary to make just small increases in Q-factor for having great reductions of THD for the filter output voltage. This result is quite important because it allows filter designer to perform a great project improvement without needing large increases in the components values.

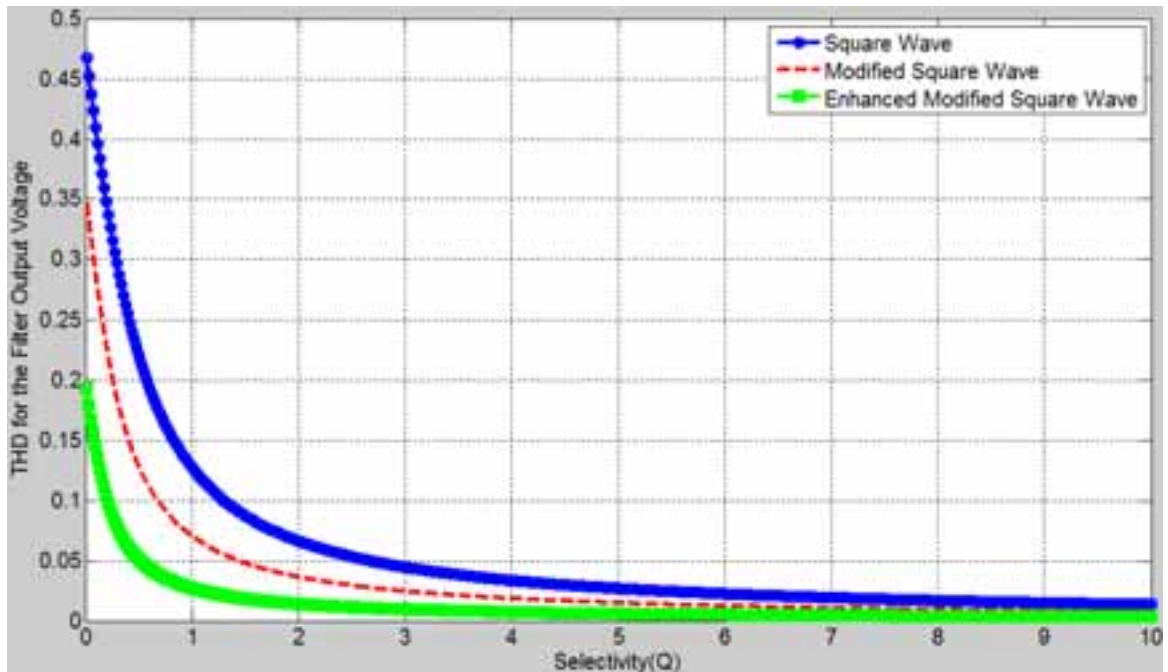


Fig. 7: THD falling for the three filtered signals plotted in linear axis

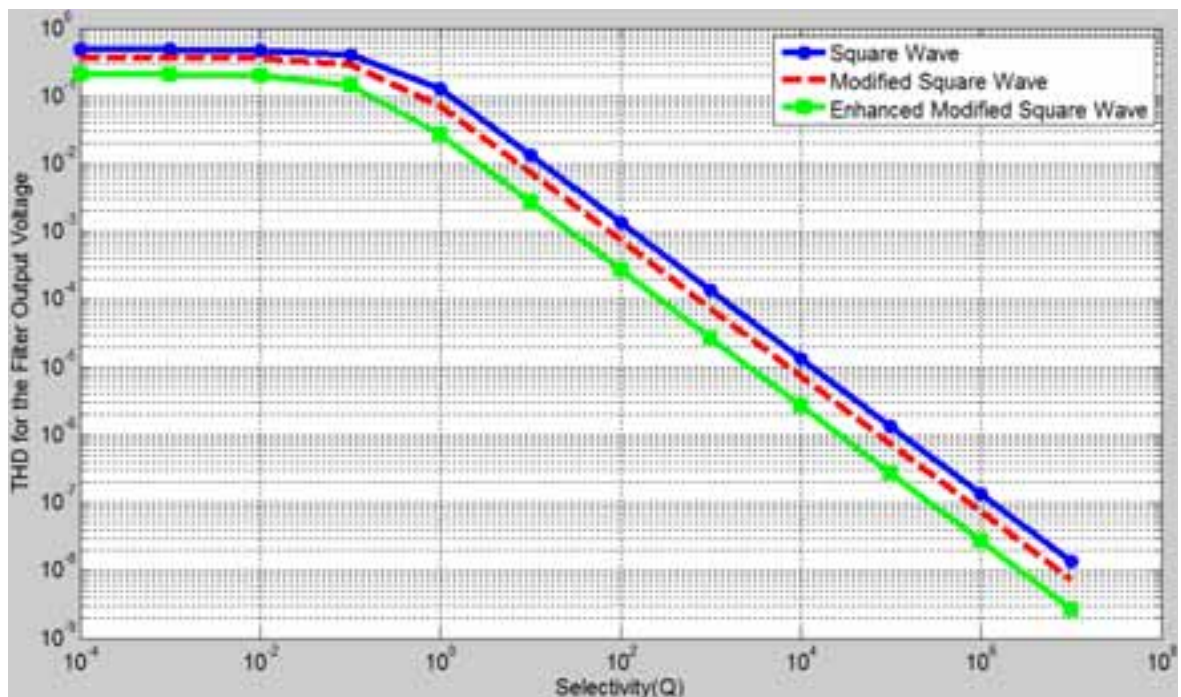


Fig. 8: THD falling for the three filtered signals plotted in logarithm axis

Fig. 8 is obtained plotting the THD for the filter output voltage versus the Q-factor in logarithm axis. This graphic shows a linear region for the three waves considered. It facilitates the possibility of proposing a mathematic equation to describe this phenomenon. However, it is beyond the scope of this paper.

## 6. Filter Efficiency and Q-factor

Since the desired is to decrease the THD, increasing the Q-factor is necessary. However, keeping the efficiency in high levels is extremely important. Therefore, the method of analysis described in previous sections is used



to observe the Filter Efficiency dependence of Q-factor. Fig 9 depicts how the filter efficiency is affected by Q-factor.

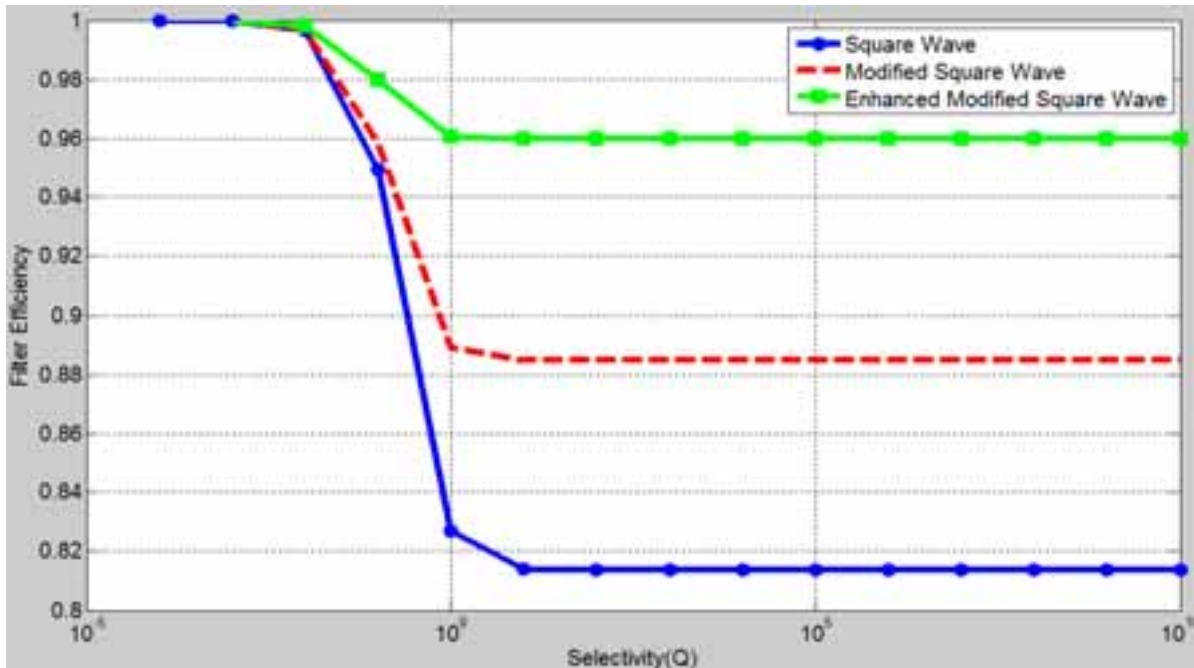


Fig. 9: Filter Efficiency falling for the three filtered signals

From graphics of Fig. 9, it is possible to notice that the Filter Efficiency decrease for the three waves when Q-factor achieves high values. However, this efficiency reduction is greater whether the input signal is either a Square-Wave or a Modified-Square-Wave, which causes high losses of energy. On the other hand, the Resonant Filter is appropriate for being coupled to an Enhanced-Modified-Square-Wave based inverter because the filter efficiency keeps near to 100%.

### 7. THD and Filter Efficiency

After analyzing the effects of Q-factor in both THD and Filter Efficiency, it is possible to make a direct comparison between them. THD and Filter Efficiency are plotted to a range of Q-factor value in Fig. 10.

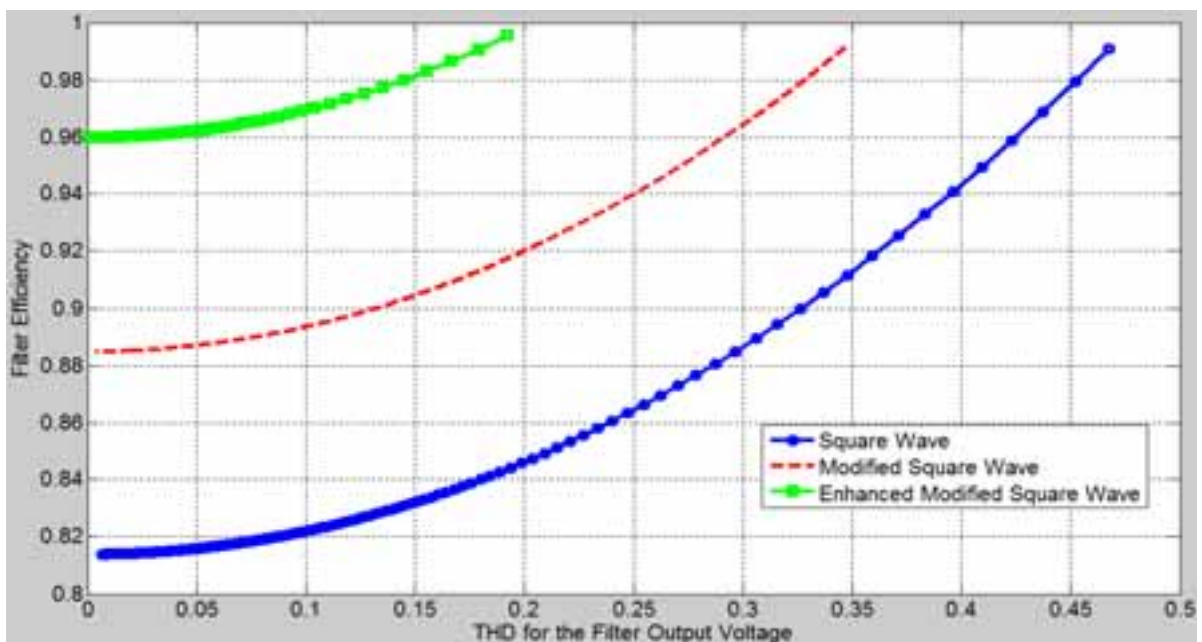


Fig. 10: Filter Efficiency vs THD for the three filtered signals

According to IEEE 519(1992) standard, the maximum value of THD that should be delivered by the system to avoid damages to the load is 5%. Table 2 shows both the Filter Efficiency and Q-factor for the three filtered

signals that provide a THD for the Filter Output Voltage accepted by the regulatory standard.

**Tab. 2: Filter Efficiency and Q-factor that provides 5% of THD**

<b>Waveform</b>	<b>Filter Efficiency</b>	<b>Q-factor</b>
<b>Square-Wave</b>	81%	2.67
<b>Modified-Square-Wave</b>	88%	1.44
<b>Enhanced-Modified-Square-Wave</b>	96%	0.5

Therefore, both Square-Wave based and Modified-Square-Wave inverters coupled to a Resonant Filter are not appropriate for applications that require THD levels near to 5% because their Efficiency decrease overly. Notice that the filter efficiency has to be multiplied by the efficiency of the other components of the system to obtain a global efficiency. However, some loads for purposes like illumination or water pumping do not require low THD levels, so a Square-Wave based inverter coupled to a Resonant Circuit can be used as part of an off-grid system to supply energy to an isolated community without damages to the loads and with low cost. On the other hand, coupling a Resonant Circuit to an Enhanced-Modified-Square-Wave based inverter is highly suitable because it is possible to reduce the wave THD from approximately 20% to 5% with an efficiency of 96% according to Tables 1-2.

## **8. Conclusion**

In this paper both THD and Efficiency analysis about a resonant circuit coupled to a classical full-bridge inverter of an off-grid PV system are performed. A resonant filter is totally defined in terms of both its resonant frequency and Q-factor. Since Q-factor represents the filter selectivity, the greater the Q-factor the lower the THD for the filter output voltage. Moreover, the Filter Efficiency decreases whether its Q-factor increases. However, both Square-Wave and Modified-Square-Wave based inverters are not suggested to be used with a resonant circuit coupled to its output when the goal is to achieve low THD values for the output voltage because the system efficiency is impaired. Finally, coupling of a resonant circuit to an Enhanced-Modified-Square-Wave is a great combination, since this system can achieve near to 100% efficiency and producing a filtered wave with low THD through low Q-factor for the RLC filter.

## **9. Acknowledgements**

This work was partially sponsored by the Undergraduate Education Decanate of the University of Brasilia.

## **10. General References**

- Amrouche, S.O., Belhamel, M., Malek, A., Maafi, A., 2007. DC/AC Solar Inverter for Solar Applications. VI World Renewable Energy Congress, 821-824.
- Banaei, M.R., Salary, E., 2011. New multilevel inverter with reduction of switches and gate driver. Energy Conversion and Management Journal, Vol. 53, Issue 2, 1129-1136.
- Castaner, L., Silvestre, S., 2002. Modeling Photovoltaic Systems Using PSpice, John Wiley and Sons, Ltd.
- Cho, K.M, Oh, W.S., Yeon, J.E., Kim, H.J, 2003. A New Switch Scheme for Resonant Inverters Using a Resonant-Frequency Tracking Algorithm. Industrial Eletronics Society, IECON '03. The 29<sup>th</sup> Annual Conference of the IEEE, Vol. 3, 2580-2585.
- Claverie, A., Courtiade, P., Venzin, P., 1994. Photovoltaic rural electrification in France. IEEE Photovoltaics Specialists Conference, Vol. 2, 2283-2286.
- Colak, I., Kabalci, E., Gazi Electrical Machines and Energy Control (GEMEC) Group, 2011. Practical implementation of a digital signal processor controlled multilevel inverter with low total harmonic distortion for motor drive applications. Journal of Power Sources, Vol. 196, Issue 18, 7585-7593.
- Dugan, R.C., McGranaghan, M.F., Santoso, S., Beaty, H.W., 2002. Electrical Power Systems Quality, McGraw-Hill Professional Engineering.

- Dunlop, J., 1997. Batteries and Charge Control in Stand-Alone Photovoltaic Systems: Fundamentals and Application, Sandia National Laboratories. Albuquerque, NM.
- Hamidat, A., Benyoucef, B., Hartani, T., 2002. Small scale irrigation with photovoltaic water pumping system in Sahara regions. *Journal of Renewable Energy*, Vol. 28, Issue 7, 1081-1096.
- Kang, F., Park, S., Cho, S.E., Kim, J., 2005. Photovoltaic power interface circuit incorporated with a buck-boost converter and a full-bridge inverter. *Applied Energy Journal*, Vol. 82, Issue 3, 266-283.
- Misak, Stanislav, Prokop, Lukas, 2010. Off-grid power systems. *International Conference on Environment and Electrical Engineering*, 14-17.
- Muljadi, E., 1997. PV water pumping with a peak-power tracker using a simple six-step square-wave inverter. *IEEE Transactions on Industry Applications*, Vol. 33, Issue 3, 714-721.
- Ofualagba, G., 2008. Photovoltaic technology, applications and market. *IEEE Power and Energy Society General Meeting – Conversion and Delivery of Electrical Energy in 21<sup>st</sup> Century*, 1-5.
- Ranjit, S.S.S., Tan, C.F., Subramanian, S.K., 2011. Implementation Off-Grid Solar Powered Technology to Electrify Existing Bus Stop. *Second International Conference on Intelligent Systems, Modeling and Simulation*, 231-234.
- Schinca, I., Amigo, I., 2010. Using renewable energy to include off-grid rural schools into the national equity project plan ceibal. *International Conference on Biosciences*, 130-134.

## **11. Standards and Survey Reports References**

- IEA PVPS Programme, 2009. Trends in Photovoltaic applications, Survey report of selected IEA countries between 1992 and 2009. IEA PVPS Programme Task 1.
- IEEE 1361™, 2003. Guide for Selection, Charging, Test, and Evaluation of Lead-Acid Batteries Used in Stand-Alone Photovoltaic (PV) Systems.
- IEEE 519, 1992. IEEE Recommended Practices and Requirements for Harmonic Control in Electrical Power Systems.